Biointerface Research in Applied Chemistry
Open-Access Journal (ISSN: 2069-5837)

Article
Volume 13, Issue 3, 2023, 263
https://doi.org/10.33263/BRIAC133.263

Enhanced Induction of MDA-MB-231 Cell Death using the Combination of Galloflavin and Electroporation

Pragatheiswar Giri [1,*], Ignacio G. Camarillo [2,3], Raji Sundararajan [1]

[1] School of Engineering Technology, Purdue University, West Lafayette, Indiana, USA; pgiri@purdue.edu (P.G.);
[2] Department of Biological Sciences, Purdue University, West Lafayette, Indiana, USA; ignacio@purdue.edu (I.G.C.);
[3] Purdue University Center for Cancer Research, West Lafayette, Indiana, USA; rsundara@purdue.edu (R.S.);
* Correspondence: raji@purdue.edu (R.S.);

Scopus Author ID 57222047471

Received: 7.03.2022; Accepted: 29.04.2022; Published: 12.06.2022

Abstract: Triple Negative Breast Cancer (TNBC) is difficult to treat since it lacks the three most commonly targeted hormone receptors. Patients with TNBC are treated with platinum core chemotherapeutics, such as Cisplatin. However, despite the anticancer effects of Cisplatin, TNBC attenuates its effect and develops a resistance eventually, which results in tumor reoccurrence. Hence, there is a critical demand for effective alternative and natural ways to treat TNBC. Towards this, inhibiting TNBC cell proliferation by blocking the key glycolytic enzyme Lactase Dehydrogenase B (LDHB) is one viable option studied in this research. Galloflavin (GF), a potent LDHB inhibitor synthesized from gallic acid, is utilized in this research. In addition, Electrochemotherapy (ECT), which involves the application of electrical pulses (EP), was utilized to enhance GF uptake. MDA-MB-231, human TNBC cells were used for this, with/out Galloflavin, and eight pulses of 600V/cm, 800V/cm, 1000V/cm, and 1200V/cm, at 100µs and 1Hz. The cells were characterized using various assays, including viability, colony-forming, and reactive oxygen species (ROS). Results indicate a TNBC cell viability of as low as 22%, demonstrating the potential of this novel treatment.

Keywords: Galloflavin; Triple Negative Breast Cancer; electrical pulses; MDA-MB-231 cells.

1. Introduction

With more than 2 million new cases of breast cancer and over 600,000 deaths in 2020, breast cancer is the most common cancer in women worldwide [1]. Out of this, 15 – 20% are TNBC [2]. TNBC lacks all the three most commonly targeted hormone receptors, namely, the estrogen receptor (ER), progesterone receptor (PR), and epidermal growth factor receptor 2 (HER2/EGFR2) amplification. Hence, there are no targeted therapies, and it is also associated with poor prognosis. The 5-year survival rate of TNBC patients is 30% compared to 66% for other breast cancer phenotypes [3]. There is a critical need for effective and alternative ways to treat TNBC. TNBC cells have distinct metabolic characteristics to support high proliferation rates [4]. They are characterized by high Lactase Dehydrogenase (LDH) enzyme levels, increasing their lactate production in aerobic and anaerobic respiration during Adenosine triphosphate (ATP) production. Lactase dehydrogenase is classified into various subunits. Among LDH subunits, LDHB is significantly upregulated during TNBC proliferation [5]. LDHB is a critical metabolic enzyme as it catalyzes the change of pyruvate to lactate in the final stage of glycolysis. ATP production in tumor cells is dependent on glycolysis and is a promising avenue to target TNBC tumor cells selectively to inhibit LDHB [6].

Towards this, Galloflavin is studied in this research. Galloflavin (3,8,9,10-tetrahydroxypyrano benzopyran-2,6-dione), a potent inhibitor of LDHB [7–10], is a natural compound identified in 1897 by German chemists Bohn and Graeb in synthesizing gallic acid with potassium hydroxide at 0°C. Gallic acid is predominantly found in green tea leaves and extract. Its molecular formulae is $C_{12}H_6O_8$ and its chemical name is 3,8,9,10-tetrahydroxy-pyrano[3,2-c][2] benzopyran-2,6-dione.

Galloflavin mainly binds to the free enzyme in the cytoplasm [11]. The binding to the free enzyme is with the help of hydrogen bonds. Galloflavin already blocks aerobic glycolysis and ATP production micromolar concentrations [12]. The inhibition of LDHB is by the binding of Galloflavin to the NADH. Galloflavin blocks aerobic glycolysis, where high differences in their energy metabolism were found in some human cancer cell lines. It also blocks the growth of cell lines resistant to other chemotherapeutics. The predominant form of action against cancer cells is apoptosis induction[11]. Galloflavin is shown to be effective in LDHB inhibition and blocks aerobic glycolysis without interfering with cell air intake and inducing cell death. Galloflavin is found to be less toxic and has the sole function of LDHB inhibition. Lethal side effects were not observed in Galloflavin. Some rare side effects may include irritation to respiratory membranes, which is harmful when in direct contact with skin and eyes [13].

To enhance GF uptake, we utilized electrical pulses (EP) to open up pores in the plasma cell membranes, which are usually nonpermeable or less permeable. This technique is known as electroporation [14–21]. This research is used to study TNBC cells, MDA-MB-231, with the combination of EP and GF. The combination of electroporation and chemotherapy can target multiple factors, in addition to opening up pores in the cell plasma membrane [11]. The controlled local administration of the electric field opens up porous layers in the cells, which temporarily converts the usually non or less permeable membrane to permeable, in a phenomenon called electroporation [12]. When electroporation is used to upload a chemodrug, it is termed Electrochemotherapy (ECT), a clinically tested and proven treatment [13–26]. It can be effective against TNBC, without causing severe toxicity and drug resistance as ECT does not rely on the receptors or hormones which target cancer cells [27-38]. Figure 1 shows the flow of action of GF, with the putative binding mode of galloflavin at the human LDH binding site [12], combined with EP for enhanced uptake that induces apoptosis.

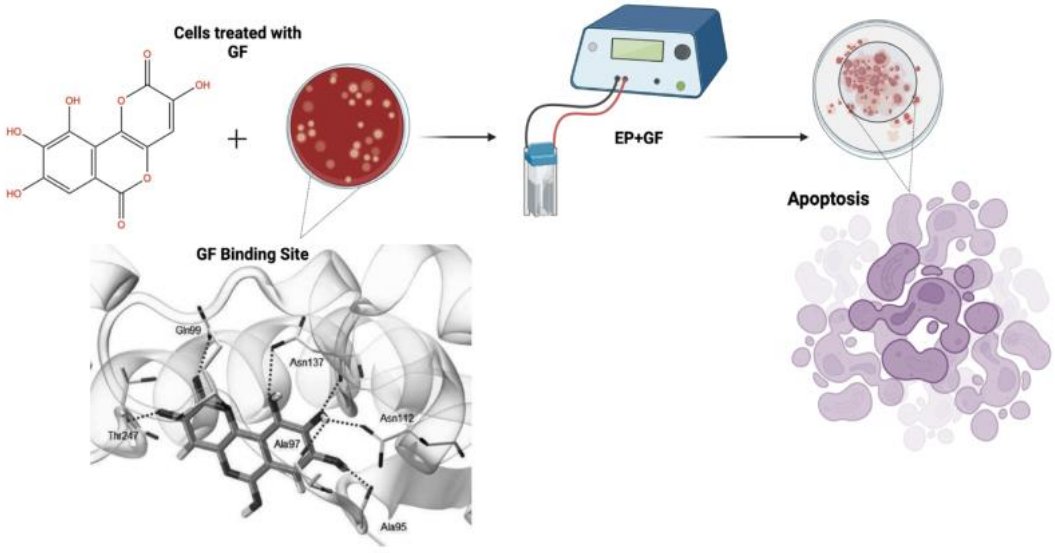

Figure 1. The flow of action of GF shown with the putative binding mode of Galloflavin, combined with EP for delivery enhancement, induces apoptosis.

2. Materials and Methods

2.1. Cell lines.

MDA-MD-231, an epithelial, TNBC cell line, first deduced from a 51-year-old Caucasian female breast cancer patient, was used. The cells were incubated and cultured in DMEM containing 10% FBS along with 1% Penicillin-Streptomycin (PS) at suitable humidity and optimal growth conditions. They were cultured in optimal growth conditions with the presence of DMEM along with 10% FBS and 1% PS [39].

MCF10A cells (non-cancerous epithelial) were cultured in optimal growth conditions with DMEM:Ham's F12 supplemented with 5% horse serum, 20ng/ml human epidermal growth factor (Sigma-Aldrich, USA), 0.5mg/ml hydrocortisone (Sigma-Aldrich), 100 ng/ml cholera toxin (Sigma-Aldrich), 10mg/ml bovine insulin (Sigma-Aldrich), 100 IU/ml penicillin and 100mg/ml streptomycin. The cells were incubated at 70%–80% humidity, 5% CO2, and 37°C [40].

2.2. Galloflavin drug.

Galloflavin (Cayman Chemical, USA) stock solution (35mM) was prepared using dimethyl sulfoxide. The stock was diluted to obtain 10-150µM Galloflavin treatment concentrations.

2.3. Electric pulse application.

A BTX ECM 830 square wave pulse generator (*Genetronics Inc. San Diego, CA, USA*) was used to apply eight unipolar, square wave pulses of 600-1200V/cm of 100µs long, at 1s intervals. The MDA-MB-231 cells were collected for electroporation at a concentration of 1×10^6 cells/ml in appropriate cell culture media and suspended at 600µl per cuvette with 4mm gap between the cuvette walls. Depending on the assay type, the collected samples were dispensed to either 96-well plates or Petri dishes [41].

2.4. MT real-time viability assay.

The Treated samples, including control (no treatment), GF only, EP only, and EP+GF, at 1 million cells/ml concentration, were seeded into 96-well plates, per Promega's protocol. The cells were supplied with 55µl of prepared media in each well. They are then incubated with optimal growth conditions for 24h. To study the cell viability, RealTime-Glo MT Cell Viability Assay (Promega, USA) was used. Synergy LX Multi-Mode Reader (BioTek Instruments, USA) was utilized for recording the luminescence (Lum). Equation 2 was used to calculate the % cell viability.

$$Cell\ Viability\ (\%) = \frac{Treated\ cell\ Luminescence\ \ value}{Control\ Luminescense} \times 100 \qquad (2)$$

2.5. Colony Forming Assay (CFA).

The MDA-MB-231 cells, after electroporation and drug treatments, were incubated with optimal growth conditions with appropriate media in 100ml Petri dishes with 1000 cells on each petri dish for a period of 9 to14 days. After the colonies were formed, they were stained

with 1.5ml of Crystal Violet (Sigma-Aldrich) and were counted using a custom MATLAB code, which thresholds, segments, and counts the number of colonies. A collection of cells of >50 cells was counted as one colony [42].

2.6. Reactive oxygen species.

Reactive species, such as free radicals and molecules from oxygen, produced in cancer cells can cause oxidative stress and cell death. Here, the reactive oxygen species (ROS) assessment at 24h was done. 20µl (20,000 cells) of treatment samples were added to a 96-well plate, with an additional 60µl of cell media. After 18h incubation, 20µl of Hydrogen Peroxide (H2O2) substrate from ROS-GloTM (Promega) was added and further incubated for six hours. The Luciferin Precursor was formed by the direct reaction between the H2O2 present in the media and the H2O2 substrate added externally from the kit. Subsequently, a 100µl luciferase detection reagent is introduced to each well, and luminescence (RLU) measurement using Synergy HTX multi-mode microplate reader is taken after 20 minutes of incubation time [43]. During that period, the Luciferin Precursor is converted to luciferin in the presence of the ROS-GloTM substrate detection solution. The H2O2 in the sample is proportional to the light signal.

2.7. Statistical analysis.

All experiments were done in triplicates. An analysis of variance was utilized to establish the significance between the different treatment data. The confidence level was set to 95% along with constant variance; data following a normal curve was confirmed before the Analysis of Variance tests.

Data from Assays were also subjected to Tukey's comparison test to establish normality and homoscedasticity in TNBC cell treatments and activities. Based on the critical value from the Tukey significance test, samples are assigned letter grades. The same letter (s) means no statistical difference, and a different letter means they are statistically different. Brown-Forsythe test was also performed along with the Analysis of Variance, which provides more robustness to the significance.

3. Results and Discussion

3.1. Dose curve.

Galloflavin causes a dose-dependent reduction of MDA-MB-231 TNBC cell viability. Figure 2 displays how cell viabilities, relative to control (normalized to 100%), decrease with respect to the different dosages of Galloflavin at 24h. The dose curve (Figure 2) indicated a cell viability drop of only 20% at 25µM (compared to control) and ranged between 75% to 85% for 25µM to 40µM. It is observed that there is steep drop-in viability after 40µM to 70%. GF at a dose of up to 125µM showed only a 40% reduction in viability, indicating that Galloflavin alone is less effective in causing cell death, necessitating the combination of the drug with an electric field for higher cell death.

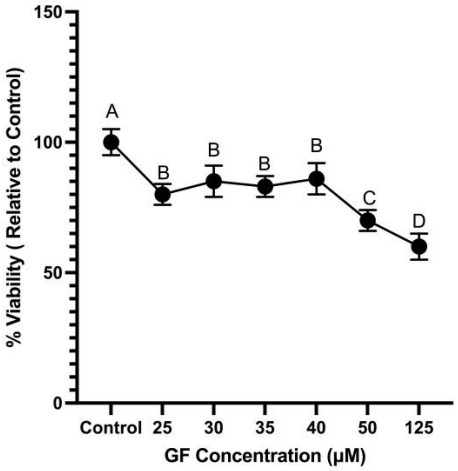

Figure 2. The dose-dependent cell viability of MDA MB 231 cells with various concentrations of (25 µM, 30µM, 35µM, 40µM, 50µM, 125µM) GF; The same letters indicate that there is no statistically significant difference between the treatments and different letters indicate a statistically significant difference.

3.2. Electrical pulse only.

Figure 3 shows the effect of electrical pulses on cell viability at 24h. As the electric field strength increases, the cell viability decreases, indicating that the electric field strength is inversely proportional to the viability of the cells-the higher the field strength, the lower the viability. There is a drop in the viability after 600V/cm and saturates after 1000V/cm. At 800V/cm, the viability was 67% relative to control (normalized to 100%) at 24h. Tukey's HSD test reveals that group means are different. The various electric field values are compared with control (at 100%), and the different letters 'A', 'B', 'C', 'D' indicate their significant differences ($P<0.05$).

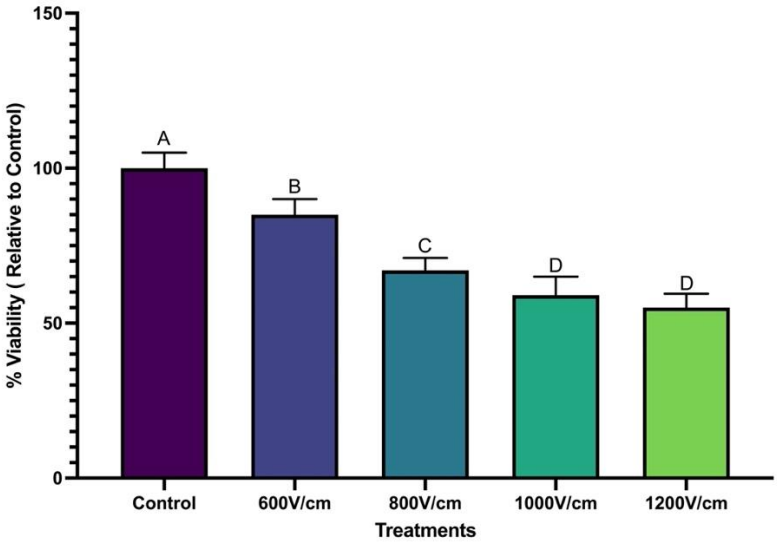

Figure 3. Viability of MDA-MB-231 when administered with electric pulses with 8 pulses of (600V/cm, 800V/cm, 1000V/cm, 1200V/cm) 100µs at 1s interval.

3.3. MT cell viability assay.

Electroporation at various voltages or GF at a dose of up to 125µM alone did not produce the desired decrease (<50%) in viability; this indicates that electric field and Galloflavin alone are less effective in killing the cells, necessitating the combination of the drug with the electric field.

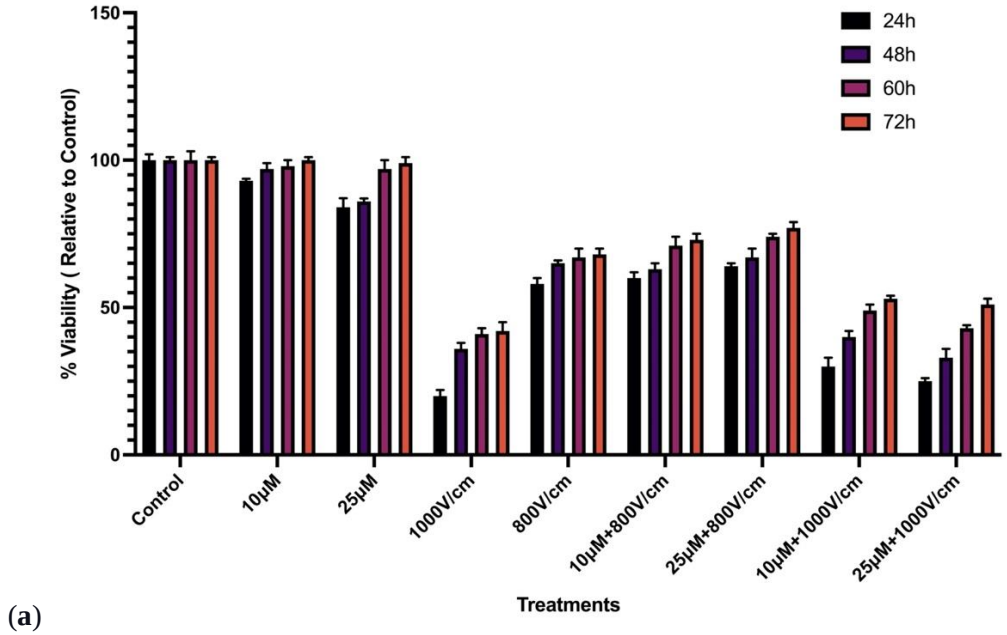

(**a**)

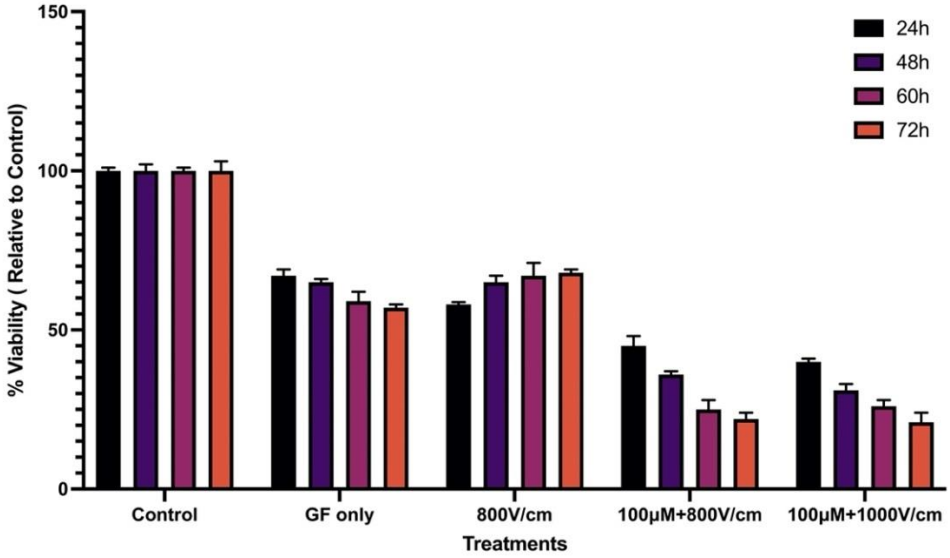

(**b**)

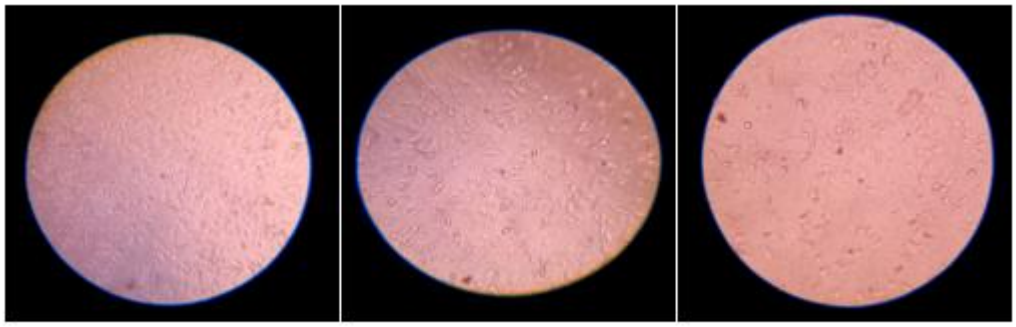

(**c**)

Figure 4. Viability of MDA-MB-231 cells at (**a**) 10μM and 25μM along with 800V/cm and 1000V/cm compared to control and drug only treatments; (**b**) 100μM+EP compared with drug only and control treatments. (**c**) MDA-MB-231 live-cell images at 24h after treatments showed (**i**) control, (**ii**) GF only, and (**iii**) EP+GF.

Figure 4a shows the viability decrease caused by the combination of Galloflavin at concentrations of 10 or 25μM, combined with 800V/cm or 1000V/cm pulses, for up to 72h (control normalized to 100%). The viability of MDA-MB-231 cells was reduced at 24h initially for all conditions. Still, they eventually increased, at 48, 60, and 72h, indicating that GF+EP

does not cause cell death over a prolonged period at the doses of 10 and 25µM. Hence, further experiments were conducted at 800 and 1000V/cm and at 100 µM combinations (Fig. 4b).

With a higher dose of 100µM and at 800V/cm or 1000V/cm, there was a consistent time-dependent decrease in cell viability associated with each combination treatment, after 24h, unlike those at lower GF concentrations. Figure 4b displays this viability decrease caused by the combination of 100µM Galloflavin with 800V/cm or 1000V/cm, at multiple time points of 24, 48, 60, and 72h. The viability decrease of the combination of Galloflavin and 800V/cm was not significantly different compared to a combination of 1000V/cm with Galloflavin. Hence, further assays were done using 800V/cm and 100µM GF.

As shown in Table 1, ANOVA analysis indicates the p-value is <0.05. This illustrates that the treatments are significantly different from each other. The Brown-Forsythe test confirms this with a P-value of 0.0192; the observed viability values are significantly different from each other. The Sum of Squares indicates the variation between individual values and the mean along with Mean Square values for error calculation.

Table 1. Summary of ANOVA analysis on MDA-MB231 cell line to assess the MT cell viability assay with all the treatments.

ANOVA table	**Sum-of-squares (SS)**	**Degree of Freedom (DF)**	**Mean Square (MS)**	**F (DF_n, DF_d)**	**P value**
Treatment	13239	4	3310	F (4, 15)=75.22	P<0.0001
Residual	660.0	15	44		
Total	13899	19			

ANOVA summary	
F	75.22
P value	<0.0001
Significant different (P < 0.05)	Yes
R squared	0.9525
Brown-Forsythe test	
F (DFn, DFd)	4.107 (4, 15)
P value	0.0192
Significantly different (P < 0.05)	Yes

Figure 4c displays the MDA-MB-231 live-cell images using a microscope at 24h after treatments (i) is control, (ii) GF only, and (iii) EP+GF. 4c (i) displays the control with the maximum number of cells among the treatments, and 4c (ii) represents the drug-only treatment, where it depicts more confluency among the MDA-MD-231 and thereby shows a lesser decrease in viability caused by 100µM GF compared to EP+GF treatment. It was observed in Figure 4c (iii) that after 24h, there was a steady decrease in cell viability associated with each combination treatment of 800V/cm with 100µM of GF.

3.4. MT cell viability assay of MCF-10A non-cancerous mammary cell line.

In order to compare the effect of this GF+800V/cm combination on nearby non-tumor cells, experiments were also conducted on the non-cancerous mammary cell line, MCF-10A. The results show (Figure 5) the regaining of MCF10A cell viability after 24h with GF only or with EP only, or with E+GF, revealing that individually, GF or EP treatments or together with both, they have only a minimal impact on non-cancerous MCF10A cell viability. It can be seen that after 48h of all treatments regained their viability, indicating the resiliency and less effect on the nearby cells due to the EP+GF treatments.

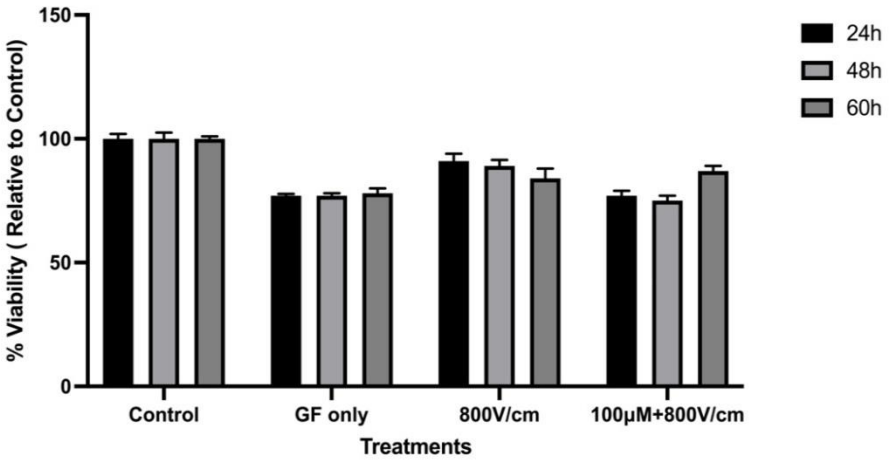

Figure 5. Viability of MCF10A at a combination of 100µM Galloflavin and 800V/cm.

ANOVA analysis, as shown in Table 2, indicates the p-value >0.05, which means that the treatments are not significantly different from each other. The Brown-Forsythe test confirms this with the P value of 0.3684 and fails to reach significant levels. The Sum of Squares indicates the variation between individual values and the mean, along with Mean Square values for error calculation.

Table 2. Summary of ANOVA analysis on the MCF10A cell line to assess the viability assay with all the treatments.

ANOVA table	**Sum-of-squares (SS)**	**Degree of Freedom (DF)**	**Mean Square (MS)**	**F (DF_n, DF_d)**	**P value**
Treatment	20111	3	315	F (3, 8) = 23	0.4636
Residual	109.3	8	13.67		
Total	1054	11			

ANOVA summary	
F	23.05
P value	>0.001
Significant different (P < 0.05)	No
R squared	0.9025
Brown-Forsythe test	
F (DFn, DFd)	1.205 (3, 8)
P value	0.3684
Significantly different (P < 0.05)	No

3.5. Cologenic assay.

Figure 6 shows the clonogenic assay results. It can be seen that the combination of 100µM Galloflavin and 800V/cm produced the least colonies (601 colonies) compared to the control (1089 colonies). 800V/cm or 100µM Galloflavin alone did not significantly reduce the number of colonies (847 and 780 colonies, respectively). The highest reduction of colonies (55% of control) was seen with the combination of drug and electroporation. The colony-forming assay results corroborated the MT cell viability results, that with the combination of EP+GF, there was maximum cell death, indicating the potency of this technique. All the treatments were done in triplicates, and the letters A, B, and C denote that they are significantly different from each other.

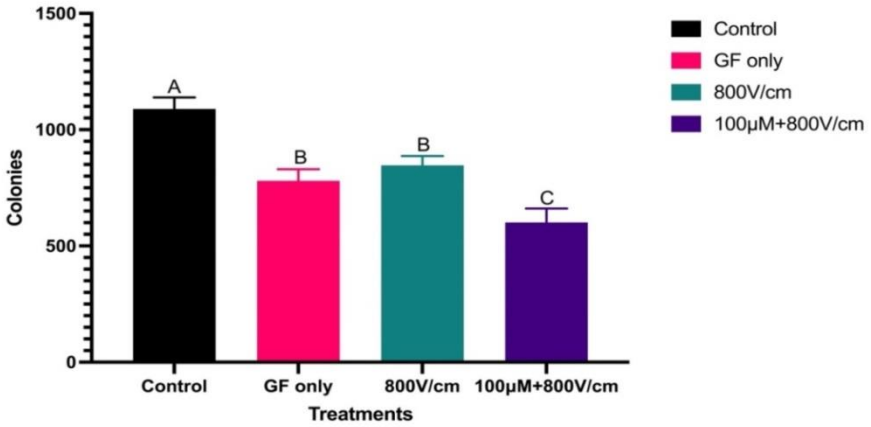

Figure 6. Colonies of MDA MB 231 cells formed with 100µM and with and without EP. The same letters indicate no significant difference between the treatments, whereas different letters indicate a statistically significant difference.

3.6. Reactive oxygen species assessment.

The quantitative results of ROS levels in the MDA-MB-231 cells are shown in Figure 7. EP at 800V/cm along with GF at 100µM produced the maximum ROS production, with more than a 4-fold increase over control. The GF-only treatment produced lower than the EP+GF combination. The EP-only treatment produced the lowest, almost at the same level as the control. The letters A, B, and C denote that they are significantly different from each other. Electroporation-only treatment does not reduce ROS levels, while the combination of E+GF treatment increased ROS production the most. This causes more oxidative stress in the MDA-MB-231 cells, leading to apoptosis [28-31].

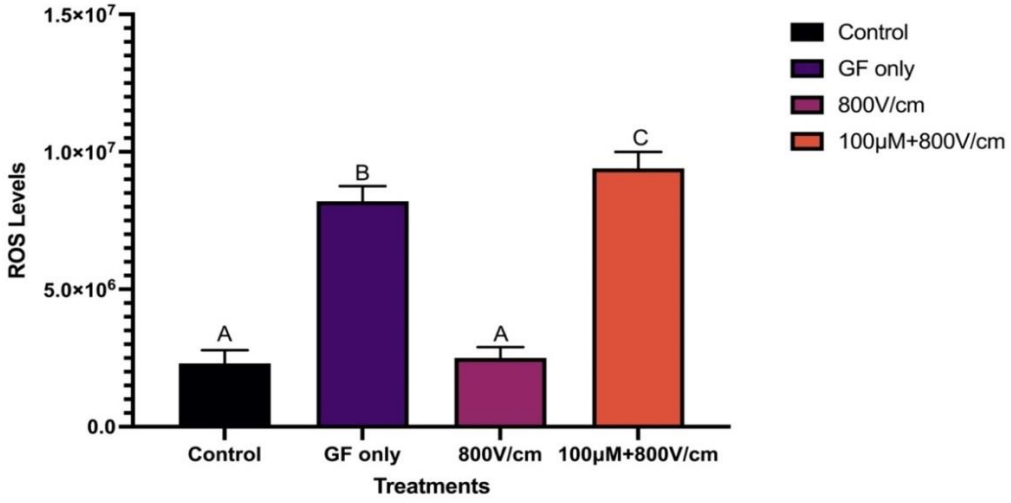

Figure 7. ROS levels for various treatments in MDA-MB-231 The letters A, B, and C denote significantly different values between treatments.

In summary, in this research, we investigated the efficacy of GF with and without electrical pulses. A comparison with the previous publication [33] indicates a very good correlation with viability at various concentrations, both at 24h and 48h (Figure 8).

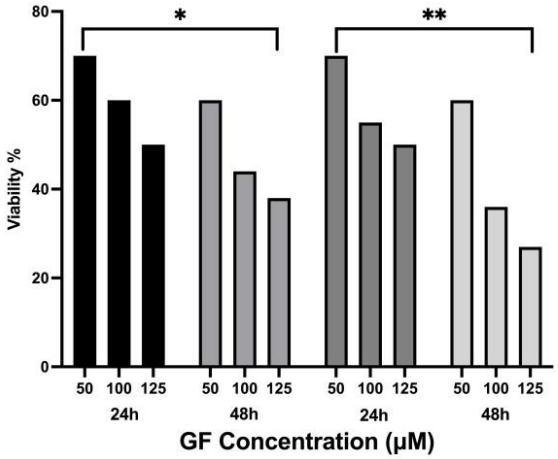

Figure 8. Comparison and good correlation of observed cell viability results (*) with the results (**) of [11].

Findings from [11] suggest that GF constitutes both anti-proliferative properties and the ability to induce cell death also suggests that 16 hours of incubation resulted in increased expression of proteins involved in apoptosis signals. All other assays corroborate these findings, indicating the efficacy of the synergy of electrical pulses and the GF, with the viability of as low as 22%.

4. Conclusions

Our results indicate that GF has the potential as an anti-TNBC agent and that EP+GF can significantly enhance cell death to reduce MDA-MB-231 cell viability and colony formation. We also observed the selectivity of this treatment mode, by showing that GF+EP does not impact non-cancerous mammary cell viability as much in TNBC cells. Further, EP+GF treatment caused increased ROS, a measure of increased cell death. In general, there were no substantial changes in viability or ROS levels when TNBC cells were treated with either GF or EP alone, indicating the potential of this novel combination treatment for possible future clinical applications.

Funding

None.

Acknowledgments

None.

Conflicts of Interest

The authors declare no conflict of interest.

References

1. Siegel, R.L.; Miller, K.D.; Fuchs, H.E.; Jemal, A. Cancer Statistics, 2021. *CA: A Cancer Journal for Clinicians* **2021**, *71*, 7–33, https://doi.org/10.3322/CAAC.21654.
2. Foulkes, W.D.; Smith, I.E.; Reis-Filho, J.S. Triple-Negative Breast Cancer. *The New England Journal of Medicine* **2010**, *363*, 1938–1948, https://doi.org/10.1056/NEJMRA1001389.
3. Dent, R.; Trudeau, M.; Pritchard, K.I.; Hanna, W.M.; Kahn, H.K.; Sawka, C.A.; Lickley, L.A.; Rawlinson, E.; Sun, P.; Narod, S.A. Triple-Negative Breast Cancer: Clinical Features and Patterns of Recurrence. *Clinical Cancer Research* **2007**, *13*, 4429–4434, https://doi.org/10.1158/1078-0432.CCR-06-3045.

4. Otto, A.M. Warburg Effect(s)—a Biographical Sketch of Otto Warburg and His Impacts on Tumor Metabolism. *Cancer & Metabolism* **2016**, *4*, 5, https://doi.org/10.1186/s40170-016-0145-9.
5. Valvona, C.J.; Fillmore, H.L.; Nunn, P.B.; Pilkington, G.J. The Regulation and Function of Lactate Dehydrogenase A: Therapeutic Potential in Brain Tumor. *Brain Pathology* **2016**, *26*, 3–17, https://doi.org/10.1111/bpa.12299.
6. Urbańska, K.; Orzechowski, A. Unappreciated Role of LDHA and LDHB to Control Apoptosis and Autophagy in Tumor Cells. *International Journal of Molecular Sciences* **2019**, *20*, 2085, https://doi.org/10.3390/ijms20092085.
7. Wendt, E.; Schoenrogge, M.; Vollmar, B.; Zechner, D. Galloflavin Plus Metformin Treatment Impairs Pancreatic Cancer Cells. *Anticancer Research* **2020**, *40*, 153-160, https://doi.org/10.21873/anticanres.13936.
8. Arundhathi, J.R.D.; Mathur, S.R.; Gogia, A.; Deo, S.V.S.; Mohapatra, P.; Prasad, C.P. Metabolic Changes in Triple Negative Breast Cancer-Focus on Aerobic Glycolysis. *Molecular Biology Reports* **2021**, *48*, 4733–4745, https://doi.org/10.1007/S11033-021-06414-w.
9. Wang, Z.H.; Peng, W.B.; Zhang, P.; Yang, X.P.; Zhou, Q. Lactate in the Tumour Microenvironment: From Immune Modulation to Therapy. *EBioMedicine* **2021**, *73*, 103627, https://doi.org/10.1016/J.EBIOM.2021.103627.
10. Mahendralingam, M.J.; Kim, H.; McCloskey, C.W.; Aliar, K.; Casey, A.E.; Tharmapalan, P.; Pellacani, D.; Ignatchenko, V.; Garcia-Valero, M.; Palomero, L.; et al. Mammary Epithelial Cells Have Lineage-Rooted Metabolic Identities. *Nature Metabolism* **2021**, *3*, 665–681, https://doi.org/10.1038/s42255-021-00388-6.
11. Farabegoli, F.; Vettraino, M.; Manerba, M.; Fiume, L.; Roberti, M.; di Stefano, G. Galloflavin, a New Lactate Dehydrogenase Inhibitor, Induces the Death of Human Breast Cancer Cells with Different Glycolytic Attitude by Affecting Distinct Signaling Pathways. *European Journal of Pharmaceutical Sciences* **2012**, *47*, 729–738, https://doi.org/10.1016/j.ejps.2012.08.012.
12. Manerba, M.; Vettraino, M.; Fiume, L.; Di Stefano, G.; Sartini, A.; Giacomini, E.; Buonfiglio, R.; Roberti, M.; Recanatini, M. Galloflavin (CAS 568-80-9): A Novel Inhibitor of Lactate Dehydrogenase. *ChemMedChem* **2012**, *7*, 311–317, https://doi.org/10.1002/cmdc.201100471.
13. Calvaresi, E.C.; Granchi, C.; Tuccinardi, T.; di Bussolo, V.; Huigens, R.W.; Lee, H.Y.; Palchaudhuri, R.; Macchia, M.; Martinelli, A.; Minutolo, F.; et al. Dual Targeting of the Warburg Effect with a Glucose-Conjugated Lactate Dehydrogenase Inhibitor. *ChemBioChem* **2013**, *14*, 2263–2267, https://doi.org/10.1002/cbic.201300562.
14. Burbach, B.J.; O'Flanagan, S.D.; Shao, Q.; Young, K.M.; Slaughter, J.R.; Rollins, M.R.; Street, T.J.L.; Granger, V.E.; Beura, L.K.; Azarin, S.M.; et al. Irreversible Electroporation Augments Checkpoint Immunotherapy in Prostate Cancer and Promotes Tumor Antigen-Specific Tissue-Resident Memory CD8+ T Cells. *Nature Communications* **2021**, *12*, 3862, https://doi.org/10.1038/s41467-021-24132-6.
15. Xu, D.; Fang, J.; Zhang, M.; Wang, H.; Zhang, T.; Hang, T.; Xie, X.; Hu, N. Synchronized Intracellular and Extracellular Recording of Action Potentials by Three-Dimensional Nanoroded Electroporation. *Biosensors and Bioelectronics* **2021**, *192*, 113501, https://doi.org/10.1016/J.BIOS.2021.113501.
16. Muralidharan, A.; Rems, L.; Kreutzer, M.T.; Boukany, P.E. Actin Networks Regulate the Cell Membrane Permeability during Electroporation. *Biochimica et Biophysica Acta (BBA) - Biomembranes* **2021**, *1863*, 183468, https://doi.org/10.1016/J.BBAMEM.2020.183468.
17. Aycock, K.N.; Zhao, Y.; Lorenzo, M.F.; Davalos, R. v. A Theoretical Argument for Extended Interpulse Delays in Therapeutic High-Frequency Irreversible Electroporation Treatments. *IEEE Transactions on Biomedical Engineering* **2021**, *68*, 1999–2010, https://doi.org/10.1109/TBME.2021.3049221.
18. Campillo-Davo, D.; de Laere, M.; Roex, G.; Versteven, M.; Flumens, D.; Berneman, Z.N.; van Tendeloo, V.F.I.; Anguille, S.; Lion, E. The Ins and Outs of Messenger RNA Electroporation for Physical Gene Delivery in Immune Cell-Based Therapy. *Pharmaceutics* **2021**, *13*, 396, https://doi.org/10.3390/PHARMACEUTICS13030396.
19. Wu, Y.; Fu, A.; Yossifon, G. Micromotor-Based Localized Electroporation and Gene Transfection of Mammalian Cells. *Proc Natl Acad Sci USA* **2021**, *118*, https://doi.org/10.1073/PNAS.2106353118.
20. Zand, E.; Schottroff, F.; Steinacker, E.; Mae-Gano, J.; Schoenher, C.; Wimberger, T.; Wassermann, K.J.; Jaeger, H. Advantages and Limitations of Various Treatment Chamber Designs for Reversible and Irreversible Electroporation in Life Sciences. *Bioelectrochemistry* **2021**, *141*, 107841, https://doi.org/10.1016/J.BIOELECHEM.2021.107841.
21. Batista Napotnik, T.; Polajžer, T.; Miklavčič, D. Cell Death Due to Electroporation – A Review. *Bioelectrochemistry* **2021**, *141*, 107871, https://doi.org/10.1016/J.BIOELECHEM.2021.107871.

22. Son, R.S.; Smith, K.C.; Gowrishankar, T.R.; Vernier, P.T.; Weaver, J.C. Basic Features of a Cell Electroporation Model: Illustrative Behavior for Two Very Different Pulses. *Journal of Membrane Biology* **2014**, *247*, 1209–1228, https://doi.org/10.1007/s00232-014-9699-z.
23. Kotnik, T.; Kramar, P.; Pucihar, G.; Miklavčič, D.; Tarek, M. Cell Membrane Electroporation - Part 1: The Phenomenon. *IEEE Electrical Insulation Magazine* **2012**, *28*, 14–23, https://doi.org/10.1109/MEI.2012.6268438.
24. Haltiwanger, S. Why Electroporation Is a Useful Technique for Cancer Treatments. In *Electroporation-Based Therapies for Cancer*; Elsevier, 2014; pp. 103–125.
25. Probst, U.; Fuhrmann, I.; Beyer, L.; Wiggermann, P. Electrochemotherapy as a New Modality in Interventional Oncology: A Review. *Technology in Cancer Research and Treatment* **2018**, *17*, https://doi.org/10.1177/1533033818785329.
26. Sersa, G.; Miklavcic, D.; Cemazar, M.; Rudolf, Z.; Pucihar, G.; Snoj, M. Electrochemotherapy in Treatment of Tumours. *European Journal of Surgical Oncology* **2008**, *34*, 232–240, https://doi.org/10.1016/j.ejso.2007.05.016.
27. Fesmire, C.C.; Petrella, R.A.; Fogle, C.A.; Gerber, D.A.; Xing, L.; Sano, M.B. Temperature Dependence of High Frequency Irreversible Electroporation Evaluated in a 3D Tumor Model. *Annals of Biomedical Engineering* **2020**, *48*, 2233–2246, https://doi.org/10.1007/S10439-019-02423-W.
28. Ozyigit, I.I. Gene Transfer to Plants by Electroporation: Methods and Applications. *Molecular Biology Reports* **2020**, *47*, 3195–3210, https://doi.org/10.1007/s11033-020-05343-4.
29. Polajzer, T.; Jarm, T.; Miklavcic, D.; Miklavčič, D. Analysis of Damage-Associated Molecular Pattern Molecules Due to Electroporation of Cells in Vitro. *Radiol Oncol* **2020**, *54*, 317–328, https://doi.org/10.2478/raon-2020-0047.
30. Graybill, P.M.; Jana, A.; Kapania, R.K.; Nain, A.S.; Davalos, R.V. Single Cell Forces after Electroporation. *ACS Nano* **2021**, *15*, 2554–2568, https://doi.org/10.1021/ACSNANO.0C07020.
31. Dermol-Černe, J.; Pirc, E.; Miklavčič, D. Mechanistic View of Skin Electroporation – Models and Dosimetry for Successful Applications: An Expert Review. *Expert Opinion on Drug Delivery* **2020**, *17*, 689–704, https://doi.org/10.1080/17425247.2020.1745772.
32. Polajžer, T.; Dermol-Černe, J.; Reberšek, M.; O'Connor, R.; Miklavčič, D. Cancellation Effect Is Present in High-Frequency Reversible and Irreversible Electroporation. *Bioelectrochemistry* **2020**, *132*, 107442, https://doi.org/10.1016/J.BIOELECHEM.2019.107442.
33. Kiełbik, A.; Szlasa, W.; Saczko, J.; Kulbacka, J. Electroporation-Based Treatments in Urology. *Cancers* **2020**, *12*, 2208, https://doi.org/10.3390/CANCERS12082208.
34. Beitel-White, N.; Lorenzo, M.F.; Zhao, Y.; Brock, R.M.; Coutermarsh-Ott, S.; Allen, I.C.; Manuchehrabadi, N.; Davalos, R. v. Multi-Tissue Analysis on the Impact of Electroporation on Electrical and Thermal Properties. *IEEE Transactions on Biomedical Engineering* **2021**, *68*, 771–782, https://doi.org/10.1109/TBME.2020.3013572.
35. Simonis, P.; Garjonyte, R.; Stirke, A. Mediated Amperometry as a Prospective Method for the Investigation of Electroporation. *Scientific Reports* **2020**, *10*, 1–8, https://doi.org/10.1038/s41598-020-76086-2.
36. Graybill, P.M.; Jana, A.; Kapania, R.K.; Nain, A.S.; Davalos, R.V. Single Cell Forces after Electroporation. *ACS Nano* **2021**, *15*, 2554–2568, https://doi.org/10.1021/ACSNANO.0C07020.
37. Dermol-Černe, J.; Pirc, E.; Miklavcic, D. Mechanistic View of Skin Electroporation–Models and Dosimetry for Successful Applications: An Expert Review. *Expert Opinion on Drug Delivery* **2020**, *17*, 689–704, https://doi.org/10.1080/17425247.2020.1745772.
38. Weaver, J.C. Electroporation of Biological Membranes from Multicellular to Nano Scales. *IEEE Transactions on Dielectrics and Electrical Insulation* **2003**, *10*, 754–768.
39. Thulasidas, J.S.; Varadarajan, G.S.; Camarillo, I.G.; Aryal, U.K.; Mittal, L.; Sundararajan, R. Proteomics Study on the Effect of Combined Treatment of Electrical Pulses and Tomato Lipophilic Extract in the Downregulation of Proliferating Cell Nuclear Antigen in Triple-Negative Breast Cancer Cell. *Phytomedicine Plus* **2021**, *1*, 100064, https://doi.org/10.1016/J.PHYPLU.2021.100064.
40. Mittal, L.; Camarillo, I.G.; Varadarajan, G.S.; Srinivasan, H.; Aryal, U.K.; Sundararajan, R. High-Throughput, Label-Free Quantitative Proteomic Studies of the Anticancer Effects of Electrical Pulses with Turmeric Silver Nanoparticles: An in Vitro Model Study. *Scientific Reports* **2020**, *10*, 7258, https://doi.org/10.1038/s41598-020-64128-8.
41. Thulasidas, J.S.; Sree Varadarajan, G.; Camarillo, I.; Mittal, L.; Sundararajan, R. Behavior of Triple Negative Breast Cancer MDA-MB-231 Cells Due to Reversible Breakdown of Cell Membrane. *2019 IEEE Conference*

on Electrical Insulation and Dielectric Phenomena (CEIDP), 20-23 October 2019, 364–367, https://doi.org/10.1109/CEIDP47102.2019.9009648.

42. Shree Thulasidas, J.; SREE Varadarajan, G.; Sundararajan, R. Pulsed Electric Field for Enhanced Extraction of Intracellular Bioactive Compounds from Plant Products: An Overview. **2019**.
43. Mittal, L.; Camarillo, I.G.; Aryal, U.K.; Sundararajan, R. Global Proteomic Analysis of Breast Cancer Cell Plasma Membrane Electroporation. *2019 IEEE Conference on Electrical Insulation and Dielectric Phenomena (CEIDP)*, 20-23 October 2019, 725–728, https://doi.org/10.1109/CEIDP47102.2019.9009762.